

# POSTER

## CARBON FIBRE REINFORCED ALUMINIUM ALLOYS MATRIX, THE STUDY OF THERMAL EXPANSION AND MECHANICAL PROPERTIES BY FINITE ELEMENT METHOD

V. Martín<sup>1</sup>, F.J. Narciso-Romero<sup>2</sup>, C. García-Cordovilla<sup>1</sup>, E. Louis<sup>1,3</sup>.

<sup>1</sup>Industria Española del Aluminio, CINDAL, Apartado 25, E-03080 Alicante (Spain)

<sup>2</sup>Departamento de Química Inorgánica, <sup>3</sup>Departamento de Física Aplicada,  
Universidad de Alicante, Apartado 99, Alicante (Spain)

### 1. INTRODUCTION

Some of the most interesting applications of aluminium carbon fibre (ACF) composites are based on the possibility to achieve controlled values for the coefficient of thermal expansion (CTE). This is required in aerospace and precision communications elements to match structural integrity. This is made by designing the contents of each material to combine the very low or negative CTE of the fiber with the value for matrix alloy.

There are many models that predict thermal expansion of carbon fiber reinforced composites. For a given composites, these models can predict quite different CTE values[1-3]. Almost all models, however, predict a value of thermal expansion coefficient that is less than that given by a simple rule of mixtures (ROM). According to ROM,

$$\alpha_c = \alpha_f V_f + \alpha_m V_m$$

where  $\alpha$  is the linear coefficient of thermal expansion,  $V$  is the volume fraction, and the subscripts,  $c$ ,  $f$ , and  $m$ , denote composite, fiber and matrix respectively. In a carbon fiber reinforced metal matrix composite, the CTE of composite is generally less than the ROM value because the presence of carbon fiber (usually with very low  $\alpha$ ) introduces a mechanical constraint on the expansion behavior of the metallic matrix (usually of high  $\alpha$ ).

In this work we have carried out finite element calculations in order to clarify the theoretical deformation characteristics of an ACF composite under thermal loads.

### 2. FINITE ELEMENT MODELLING

Finite element modelling (FEM), has proven a powerful method for the understanding of microstructural behavior of composites [4,5]. The method uses a numerical approach to solve the structural equations. Thermally induced deformation is simply taken into account by means of the inclusion of a thermal strain  $\epsilon^{th}$  to the total elastic strain in the form:

$$\{\epsilon^{th}\} = \Delta T [\alpha_x \alpha_y \alpha_z 000]^t$$

A 3D unit cell of an idealized ACF has been modelled as shown in Figures 1 and 2 (Due to the symmetric nature of the domain, only an eighth is shown). The mesh has a finer structure in the vicinity of the fiber and 285 8-node hexahedral anisotropic elastic elements were used.

Material properties are chosen perfectly elastic and independent of temperature as in Table 1, and an uniform thermal load of 10 K has been imposed and thermal displacement calculated.

Calculations have also been made considering a change in

Young modulus of matrix from 70 to 50 GPa

### 3. RESULTS AND DISCUSSION

As can be seen in Figure 3, deformation is not homogeneous in the domain modelled. Calculation of CTE using mean displacement of the domain yields to a value of CTE of  $16.82 \cdot 10^{-6} \text{ K}^{-1}$ . Using ROM technique, the value is  $20.82 \cdot 10^{-6} \text{ K}^{-1}$ . Modification of Young modulus yields to a CTE of  $15.42 \cdot 10^{-6} \text{ K}^{-1}$ .

Mechanical linkage between matrix and reinforcement in aluminium composites has been extensively reported in the past. Also, changes in structural composite performance due to differences in mechanical behavior between reinforcement and matrix phases have been micromechanically modelled [2]. As can be seen, ROM calculated value corresponds with the one obtained if we suppose that matrix and reinforcement deform independently. If there is a mechanical link between both, ROM value is no longer valid.

Inhomogeneous deformation reduces CTE value, as the deformation of one phase is constrained by the other one. Figure 4 shows the differences in thermal deformation of x-axis for the three models. Inclusion and modification of mechanical properties has an important effect on shape change of cell.

Mechanical linkage between matrix and fibre, also induce fiber size and geometrical effects that are not taken into account by ROM modelling. Inclusion of plasticity, and more complex mechanical behavior of matrix and fiber should lead to more accurate microscopic descriptions.

### 5. CONCLUSIONS

This results show that mechanical interaction between matrix and fibers induce modifications to the value of CTE calculated with ROM. Prediction of CTE values is only possible if accurate micromechanical models are available.

### 6. REFERENCES

1. J.J. Masson, K. Weber, M. Miketta, K. Schutle, 12<sup>th</sup> Risø International Symposium on Materials Science, 509 (1991), Roskilde Denmark.
2. K. Schmidt, C. Zweben, R. Arsenault, "Thermal and Mechanical Behavior of Metal Matrix and Ceramic Matrix Composites", Ed. ASTM, 155 (1990).
3. T. A. Hahn, "Metal Matrix Composites: Mechanism and Properties", Academic Press, 329 (1991).
4. H. Zhang, P.M. Anderson, G.S. Daehn, Metallurgical and Materials Transactions A, **25A**, 415 (1994).

2. K. Schmidt, C. Zweben, R. Arsenault, "Thermal and Mechanical Behavior of Metal Matrix and Ceramic Matrix Composites", Ed. ASTM, 155 (1990).  
 3. T. A. Hahn, "Metal Matrix Composites: Mechanism and Properties", Academic Press, 329 (1991).

4. H. Zhang, P.M. Anderson, G.S. Daehn, Metallurgical and Materials Transactions A, **25A**, 415 (1994).  
 5. H. Zhang, G.S. Daehn, R.H. Wagoner, Scripta Metallurgica et Materialia, 24, 2151 (1990)

Table 1. Materials properties used in the models

Materials	Type	Mechanical Properties			Thermal Properties	
		$E_{x,y}$ (GPa)	$E_z$ (GPa)	$\eta$	$\alpha_{x,y}$ ( $10^{-6}K^{-1}$ )	$\alpha_z$ ( $10^{-6}K^{-1}$ )
Matrix Reinforc.	AA6061	70	70	0.3	23.6	23.6
	P100	50	500	0.2	40	-1.5

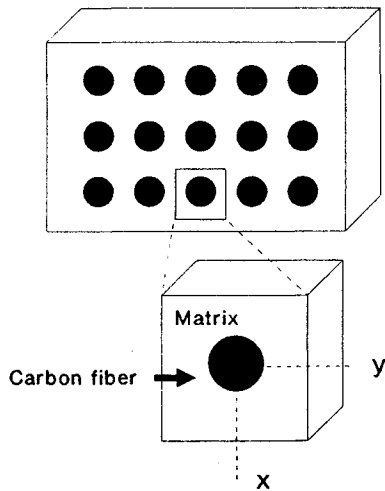


Figure 1. Schematic diagram of the carbon fiber reinforced metal matrix composite.

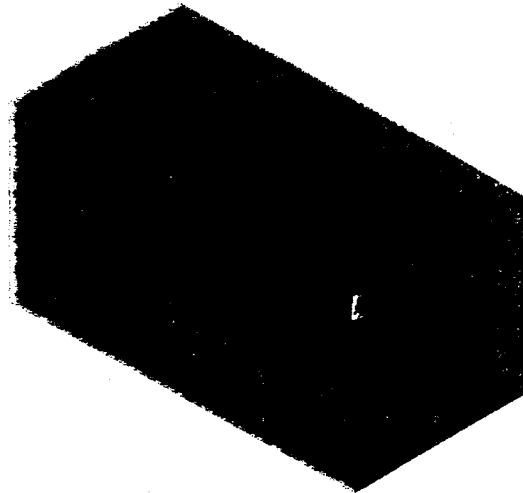


Figure 2. Meshing of the unit cell.

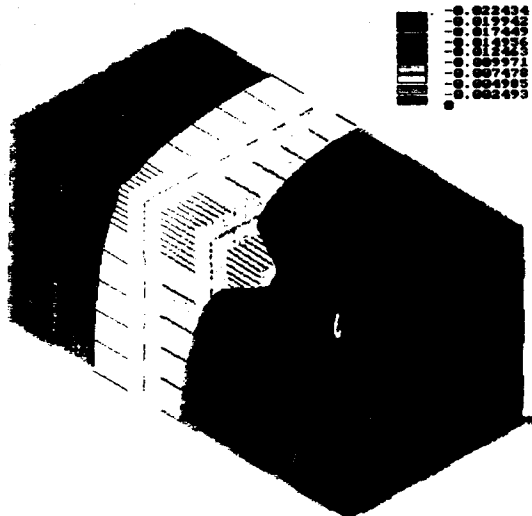


Figure 3. Distribution of thermal deformation in the model.

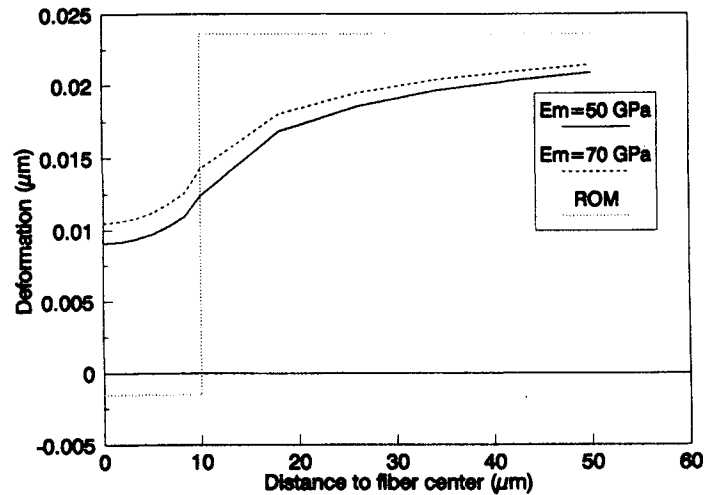


Figure 4. Amount of the deformation of x-axis for the three models